THE INFLUENCE OF PYROGENIC NANOSILICAS WITH DIFFERENT SURFACE AREAS AND AGGREGATION STATES ON CEMENT HYDRATION

A. Bagheri[a], T. Parhizkar[b], H. Madani[*c] and A. Raisghasemi[b]
[a]Civil Engineering Faculty, K.N.Toosi University of Technology, No. 1346, Vali Asr Street, Mirdamad Intersection, Tehran, Iran.
[b]Department of Concrete Technology, Building and Housing Research Center (BHRC), Pas Farhangian Street, Sheikh Fazlollah Express Way, Tehran, Iran.
[c]Civil Engineering Faculty, Kerman Graduate University of Technology, Haftbagh Alavi Express Way, Kerman, Iran.

ABSTRACT

In this study, the pozzolanic activity of pyrogenic nanosilicas with different specific surface areas ($90m^2/g$, $200m^2/g$ and $300m^2/g$) and aggregation states in lime and cement pastes and their effects on cement hydration have been investigated and compared to the influences of silica fume. The results show very rapid pozzolanic activity for the pyrogenic nanosilicas compared to silica fume and the rate increases with increasing specific surface area of nanosilicas. The large differences in the initial aggregate sizes of nanosilicas appear not to influence their pozzolanic activity. Nanosilicas accelerate cement hydration at early ages, however; at later ages, progress in cement hydration is reduced.

1. INTRODUCTION

In recent years by development of nanoscience and due to structural similarities with silica fume, a considerable research effort has been attracted to the investigation of the influence of nanosilicas on the properties of cement-based materials. However, unlike silica fume, which is a by-product of a specific metallurgical process, nanosilica materials can be produced by a variety of methods yielding different characteristics. In a general classification, the main types of nanosilicas, which have been used in cementitious systems

---

* E-mail address of the corresponding author: h.madani@kgut.ac.ir (H. Madani)

by various researchers can be divided into, nanosilica sols, pyrogenic nanosilicas, nanosilica gels and precipitated nanosilicas.

In a recent study, it was shown that the rate of pozzolanic reactivity of monodispersed nanosilica hydrosols is mainly dependent on their specific surface area [1]. However, compared to the monodispersed nanosilica sols, the other types of nanosilicas are in the form of aggregated particles. For instance, the pyrogenic nanosilicas are in the form of large agglomerates with dimensions mainly greater than one micrometer [2]. It is not clear that like monodispersed nanosilica sols, the rate of pozzolanic reactivity of aggregated nanosilicas is controlled by their specific surface area or the aggregation status of these materials is the main factor which controls their rate of pozzolanic reactivity. Hence, more concentrated studies are required on aggregated forms of nanosilicas to characterize their behavior in cementitious mixtures. The current study is thus focused on the pyrogenic nanosilicas as one of the main types of aggregated nanosilicas.

The pyrogenic nanosilicas are generally produced through reaction of silicon tetrachloride, hydrogen and oxygen in high temperature furnaces [2-4]. They can be produced with different specific surface areas ranging from about $50m^2/g$ to $400m^2/g$ [4]. In the production process of these materials, the particles fuse together and form primary aggregates with dimensions up to a hundred nanometers. The primary aggregates also bind together and form agglomerates up to about a few hundred micrometers in length [2-5].

Several studies have investigated the pozzolanic reactivity of pyrogenic nanosilicas and their influence on the early hydration characteristics of cement mixtures [6-10]. Unfortunately, in these researches, the effect of specific surface area and aggregation status of pyrogenic nanosilicas on their pozzolanic reactivity were not investigated. It is also notable that although initial acceleration of cement hydration due to incorporation of nanosilicas is generally agreed upon [6-12], cement hydration after early ages has not been adequately characterized.

This study was conducted in order to help with the characterization of the influence of the pyrogenic nanosilicas on the properties of cement composites, taking into account the effect of parameters such as specific surface area and the aggregation state of nanosilicas. The pozzolanic reactivity of the pyrogenic nanosilicas with different surface areas in lime pastes with water/solids ratio of 2 and in cement pastes with water/solids ratio of 0.27 was investigated from a few hours up to 100 days. In order to study the aggregation status of the pyrogenic nanosilicas in the environment of cement based mixtures, the influence of Calcium ions on the aggregation status of the nanosilicas was investigated and the results were compared with the size distribution of these materials in their initial suspensions. The effect of the pyrogenic nanosilicas with different specific surface areas and cement replacement levels on the setting times of the cement pastes was also investigated.

2. MATERIALS AND METHODS

2.1. Materials and apparatus
Three types of pyrogenic nanosilicas with different specific surface areas including; Aerosil 90, Aerosil 200 and Aerosil 300 supplied by Degussa Corporation were used in this study. These

products according to the manufacture's data have surface areas of 90, 200 and $300\,m^2/g$ and mean particle sizes of 20, 12 and 7 nm, respectively. The silica fume used with a specific surface area of $21\,m^2/g$ was supplied by Azna Ferroalloy Company and complied with requirements of ASTM C1240 [13].

Before introducing nanosilicas into lime or cement pastes, these materials were initially mixed with water in mass concentration of 15% or 10%, the required amounts of NaOH for adjusting the pH of suspension to 10 was added, and the suspensions were mixed for 1 hour with a 3000rpm high shear mixer. The nanosilica suspensions utilized in lime pastes had a mass concentration of 15%. The aqueous suspensions of Aerosil 200 and Aerosil 300 prepared for use in cement pastes had a mass concentration of 10%. The aqueous suspension of Aerosil 90 used in cement paste was the same as the suspension used in lime paste. It should be noted that increasing the pH could enhance the repulsive electrostatic forces between particles, resulting in a finer aggregation status [2,14].

To utilize silica fume in pastes, this material was mixed with water in mass concentration of 30% with a high shear mixer for 4 minutes. In this research, the codes S90, S200, S300 and SM are used to denote suspensions containing Aerosil 90, Aerosil 200, Aerosil 300 and Silica fume (Microsilica), respectively. In this respect, for instance, S200-10% and S200-15% represent the aqueous suspensions containing Aerosil 200 with mass concentrations of 10% and 15%, respectively.

The cement used was a type II Portland cement complying with the requirements of ASTM C150. The physical and chemical properties of the nanosilicas, silica fume and cement are shown in table1. The Calcium Hydroxide with a purity of more than 98% was supplied by Merck Corporation.

Table 1: Chemical composition and physical properties of cement, silica fume and pyrogenic nanosilicas

Properties	Cement	Silica fume	Aerosil 90	Aerosil 200	Aerosil 300
Silica (SiO_2)	22.2	92.3	99.8<	99.8<	99.8<
Iron oxide (Fe_2O_3)	3.24	1.0	-	-	-
Alumina (Al_2O_3)	4.63	1.3	-	-	-
Calcium oxide (CaO)	61.88	1.6	-	-	-
Magnesium oxide (MgO)	3.93	0.9	-	-	-
Sulfur trioxide (SO_3)	1.86	0.11	-	-	-
Sodium oxide (Na_2O)	0.28	0.25	-	-	-
Potassium oxide (K_2O)	0.57	0.79			
Loss on ignition	1.02	1.53	<1	<1	<1
Moisture content	0.3	0.2	<1	<1.5	<1.5
Surface area(m^2/g)	0.314	21	90	200	300
Particle size (nm)	-	-	20	12	7
Abbreviation	-	M	A90	A200	A300

2.2. Particle size distribution

The particle size distributions of the aqueous suspensions of pyrogenic nanosilicas were determined by particle size analyzer Mastersizer 2000 (Malvern Instruments) designed for particles in the size range 20 nm to 2 mm. The instrument employs Mie theory to calculate

particle size distributions from the scattered laser light.

In order to investigate the influence of Calcium ions on the aggregation status of pyrogenic nanosilicas, 0.75g Calcium Hydroxide (CH) was mixed with 50g water. Then, 500g of suspension S200-10% (or S300-10%) was added to the CH mixture. The resulting suspension was mixed by a low shear mixer with rotating speed of 200 rpm for 3min. Afterwards, the particle size distribution was determined using Mastersizer 2000. The influence of Ca^{2+} ions on the coagulation of Aerosil 90 was also investigated. For this purpose, initially 0.75g Calcium Hydroxide was mixed with 217g water. Then, 333g suspension of S90-15% was added to the CH mixture and the suspension was mixed using the low shear mixer with rotating speed of 200rpm for 3min. In this study, the mass ratio of Calcium ions to nanosilica and water was adjusted to 0.8% and 0.08% (0.8g/lit), respectively. It should be noted that the saturation level of Ca^{2+}, which is obtained at the end of pre-induction period [15], is about 20mmol/lit, which is equal to the value used in this study.

2.3. Mixture proportions and specimen preparation

Lime pastes were prepared by mixing of hydrated lime with the nanosilicas or silica fume in mass ratio of 1.85 (molar ratio of 1.5) and water to solid ratio of 2. The pastes were mixed in a mechanical mortar mixer for 3 minutes followed by 1 minute stopping and further 3 minutes of mixing. The specimens were cast into plastic bottles, which were sealed airtight and were allowed to react at a temperature of about 23±2 °C for designated periods of time. Prior to the thermogravimetric tests, the specimens were washed by acetone and were dried under N_2 flow.

The cement pastes were prepared at a water to solids (cement + nano silica or silica fume) ratio of 0.27. The water content of the nanosilica suspensions was considered as a part of mix water. The replacement levels of cement by the solid content of the nanosilicas were (i) 1, 2, 3 and 5% for A90 (ii) 1, 2 and 3% for A200 and (iii) 1, 2 and 3% for A300. Higher replacement levels were not considered because of severe reduction of flowability. A control paste containing only cement and cement pastes with 1, 2, 3, 5 and 7.5 % of cement replaced by silica fume were also made for comparison purposes. No dispersing agent was used in production of the cement pastes.

The cement pastes were mixed in a mechanical mortar mixer for 3 minutes followed by 1 minute stopping and 4 minutes of further mixing. Specimens were cast in 50×50×50 steel molds in two layers with tamping of 32 tamps per layer followed by 10s vibration at the end. Afterwards the cast specimens were covered to minimize water evaporation. The molds were stripped after 24 h, and the specimens were immersed in water (CH-saturated) at 23±2 °C until testing.

At predetermined ages, the core of the cement paste sample containing 3%(wt) of nanosilicas and silica fume was crushed and the hydration was stopped by immediate washing the sample with acetone and oven drying at 105°C for 18 hours.

The codes A90, A200, A300 and M are used to denote cement mixtures containing Aerosil 90, Aerosil 200, Aerosil 300 and Silica fume (Microsilica), respectively. Therefore, the cement paste of A200-3% represents the cement paste incorporating 3% of Aerosil 200 (solid content).

2.4. Determination of the pozzolanic reactivity of the nanosilicas and Silica fume in the lime and cement pastes

At required ages (3.5hour and 1, 3, 7, 28 and 100 days) thermal analysis (TGA/DSC) was performed on dried samples to evaluate the pozzolanic reactivity of the nanosilicas and silica

fume in their respective lime pastes. Thermal analyses (TGA/DSC) were conducted by a NETZCH STA449C instrument on 50-75 mg of the dried paste samples in N_2 atmosphere. The samples were heated to 1005°C at a heating rate of 10°C/min; consequently, considering any carbonation effect, the pozzolanic reactivity was determined as the ratio of the consumed CH to the initial CH. The DSC graphs were used to determine the onset and the end of decomposition of CH.

For the cement pastes containing 3% of the nanosilicas or silica fume and the plain paste, weight loss due to Calcium Hydroxide (CH) decomposition is estimated by the TG graphs. The CH contents of cement pastes at ages of 1, 3, 7, 28 and 100 days were determined by considering the carbonation effect. The DSC graphs were used to determine the onset and the end of decomposition of CH. In order to account for slightly lower cement content of pastes containing the nanosilicas and silica fume compared to the plain paste, the CH content of the pastes incorporating these materials was normalized with respect to the cement content of the plain paste, using the following formula:

$$CH_{norm}(t) = \frac{CH(t)}{m_c \times CH_{plain\ paste}(t)}$$ (1)

m_c: the mass ratio of cement to cementitious materials.
$CH_{plain\ paste}(t)$: CH content of plain paste at any time t (g/g of ignited weight).
$CH(t)$: CH content of paste at time of t (g/g of ignited weight).

CH_{norm}: normalized CH with respect to CH of plain paste.

2.5. Determination of the degree of hydration of cement in the cement pastes

TGA/DSC was used to determine the evolution of the nonevaporable water content $W_n(t)$ in the cement pastes during hydration. The non-evaporable water content (W_n) was obtained as the difference in mass between the sample heated at 105°C and 1005°C normalized by the mass after heating to 1005°C. The nonevaporeable water was corrected by considering the carbonation effect. In this study, it was assumed that siliceous materials (nanosilicas and silica fume) do not bind water chemically in reaction with Calcium Hydroxide and the resulting C-S-H has the same bound water content as Calcium Hydroxide. This assumption had been used by several studies such as [1, 16-17]. It was also assumed that the hydration of 1g cement produces about 0.23g non-evaporable water [18].

The following formula is used to calculate the hydration degree of cement:

$$Hydration\ degree\ of\ cement = \frac{W_n(t)}{m_c.W_n(\infty)} \times 100$$ (2)

$W_n(t)$: The non evaporable content of cement paste at any time t.

$W_n(\infty)$: The non evaporable water content at $t \rightarrow \infty$ corresponding to full hydration of 1 g of cement.

$mc =$ The mass ratio of cement to cementitious materials

2.6. Setting times
A standard method for assessing the setting time of cement pastes is the Vicat test described in ASTM C191 [18]. The test consists of measuring the penetration depth of a standard needle, which falls down under gravity. Initial setting time is when the needle penetration is 25 mm±0.5 mm and the final setting time corresponds to less than 0.5 mm of penetration. In the standard method, the cement paste is required to be at the normal consistency. In this study, the procedure was modified and the cement pastes were prepared according to the composition described earlier without attempting to achieve normal consistency. The reason being, the Vicat test is used here to compare the setting time of various cement pastes with and without nanosilicas at a constant water to cementitious materials.

3. RESULTS AND DISCUSSION

3.1 Particle size distribution of aqueous suspensions of pyrogenic nanosilicas
In order to help with the dispersion of the pyrogenic nanosilicas in the aqueous medium, the pH of suspensions was adjusted to 10 and the suspensions were mixed for 1 hour by a high shear mixer with a rotating speed of 3000rpm. By increasing the pH, the surface silanol groups are dissociated according to the following formula, resulting in higher negative charges at the surface of nanosilica particles and consequently higher double layer electrostatic forces between particles [2,14,20-24]. Enhancing the amount of electrostatic forces between particles could provide a more stable and finer aggregation status for the pyrogenic nanosilicas in the aqueous medium.

$$Si\text{-}OH + OH^- \rightarrow Si\text{-}O^- + H_2O \qquad (3)$$

The particle size distributions of the nanosilica suspensions before their use in cement pastes and lime pastes are presented in Fig. 1. The suspensions intended for use in the cement pastes were S300-10%, S200-10%, S90-15% and SM-30%. As it is shown in Fig. 1, the median particle size of suspension SM-30%, S90-15%, S200-10% and S300-10% were 106 μm, 0.27 μm, 0.135 μm and 22.8 μm, respectively. Therefore, it appears that the aggregate dimensions of the microsilica and nanosilica suspensions intended for use in cement mixtures increases in the order: (SM-30% > S300-10% > S90-15% > S200-10%).

The suspensions SM-30%, S90-15%, S200-15% and S300-15% were intended for use in the lime pastes. The median size of aggregates of SM-30%, S90-15%, S200-15% and S300-15% were found to be 106μm, 0.27μm, 0.28μm and 26.6μm, respectively. As can be seen in Fig. 1 the dimensions of microsilica and nanosilica materials intended for use in lime pastes increases in the order, SM-30% > S300-15% > S200-15% > S90-15%.
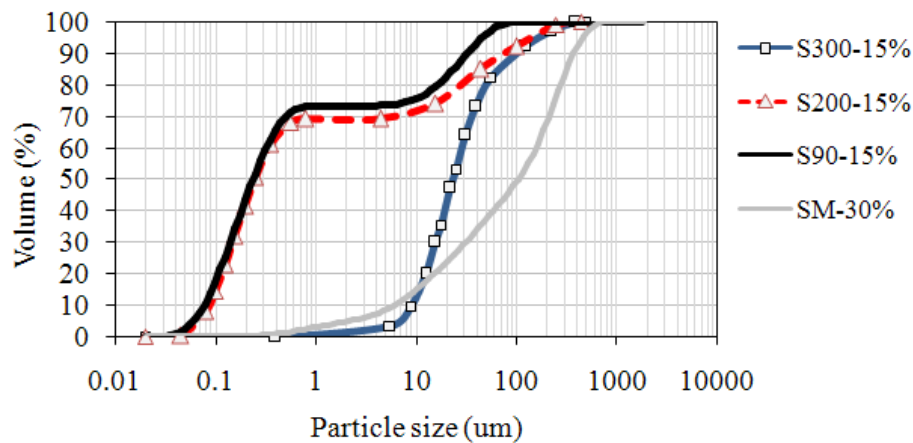
3.2. The pozzolanic reactivity of the nanosilicas and silica fume in lime pastes
The pozzolanic reactivity of the pyrogenic nanosilicas with different specific surface areas and silica fume are presented in Fig. 2. The results indicate that, at the first 3.5 hour, A300 consumed about 80% of lime. This content is comparable with the pozzolanic reactivity of A200 at 24 hour, A90 at 96 hour and silica fume at 28days. At 24 hours, the pozzolanic reactivity of A300 was nearly completed, whereas the similar content of the lime consumption was obtained after 3 days for A200, 28 days for A90 and 100days for silica fume. At 100 days, all the nanosilicas had almost the same pozzolanic reactivity and consumed more than 98% of lime. The amount of

combined lime by silica fume at the age of 100 days was slightly lower than that observed for the pyrogenic nanosilicas, however it appears all the materials investigated have similar pozzolanic reactivity in the longer time.
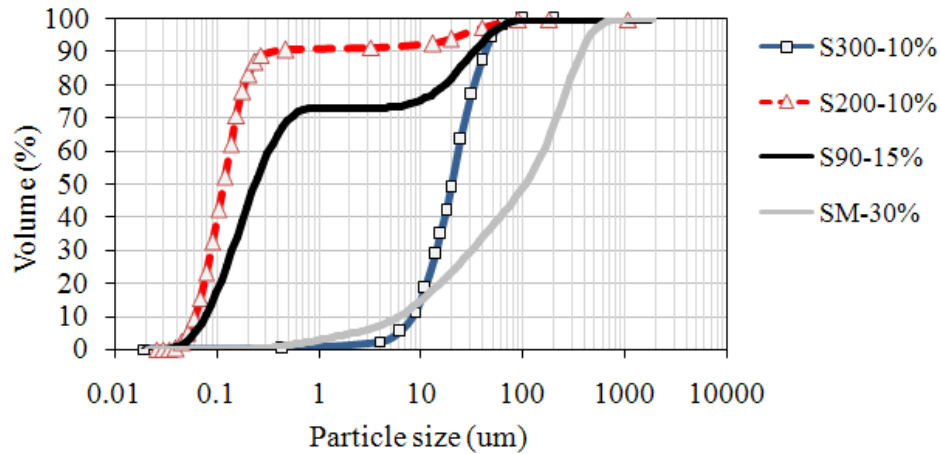
(a)

(b)

Figure 1. Size distributions of the aqueous suspensions of silica fume and pyrogenic nanosilicas intended to be used in, (a) Cement pastes and (b) Lime pastes

The results indicate that like monodispersed nanosilica sols the rate of pozzolanic reactivity of the nanosilicas mainly depends on their specific surface area and the nanosilicas with higher specific surface areas have higher rates of lime consumption, especially at early ages.
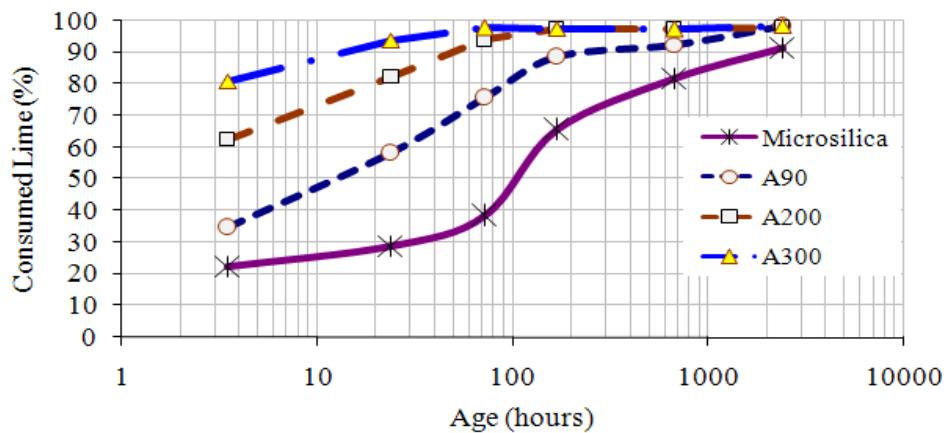
Figure 2. The pozzolanic reactivity of the nanosilicas and silica fume in the lime pastes

3.3. The pozzolanic reactivity of the nanosilicas and silica fume in cement pastes

The Calcium Hydroxide contents of the cement pastes containing nanosilicas and silica fume at 3% cement replacement, at various ages, are presented in Fig. 3. In order to account for the slightly lower cement content of pastes containing the pozzolans, the normalized Calcium Hydroxide contents based on equal cement level are given in Fig. 4.

   The results show that the pozzolanic reactivity of the nanosilicas began within the first day, while silica fume did not have significant pozzolanic reactivity until 3days. The results also indicate the nanosilicas with higher surface areas had more lime consumption than those with coarser particles and this effect is more pronounced at early ages. This confirms the dependence of the pozzolanic reactivity of the pyrogenic nanosilicas on their specific surface area.
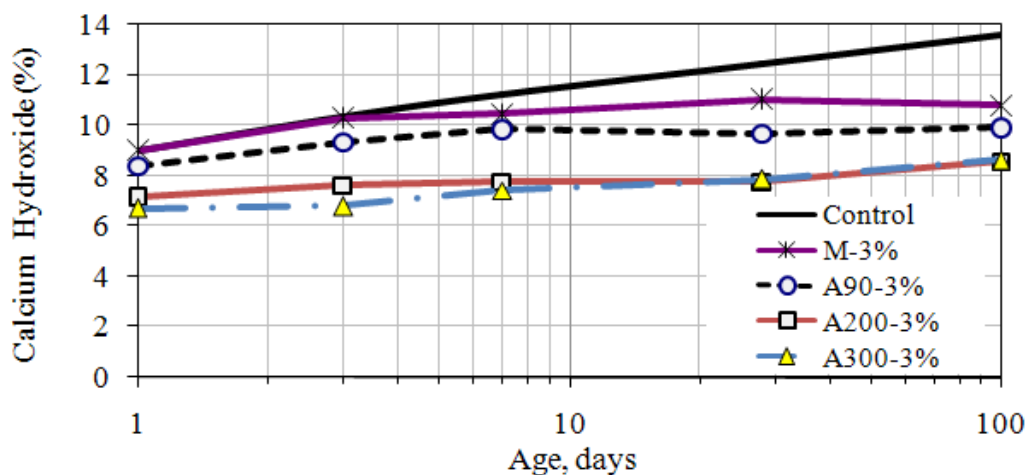

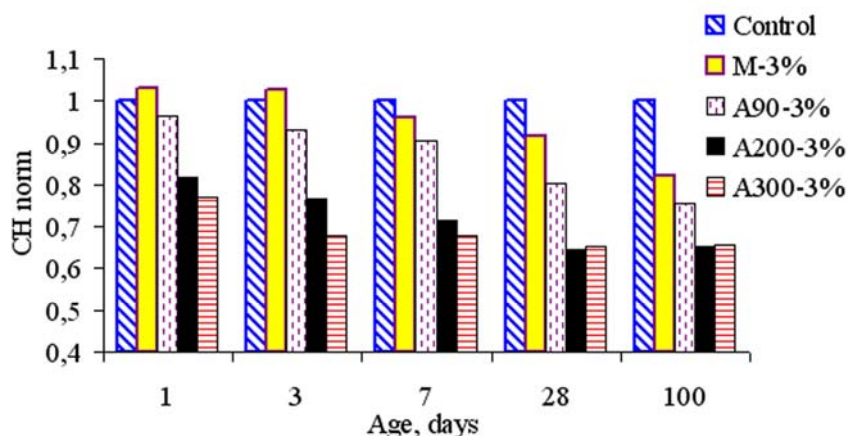Figure 3. Lime content of cement pastes

Figure 4. The normalized lime content of the cement pastes with nanosilicas and silica fume

It is interesting that aggregates of Aerosil 300 are introduced into the lime and cement pastes with median dimensions greater than 100 times than that of the aggregates of Aerosil 200. The aggregates of Aerosil 90 were also significantly smaller than the aggregates of Aerosil 300. However, when the rate of lime consumption of the nanosilicas is compared, it is found that despite the vastly different initial aggregation state of the nanosilicas, their rate of pozzolanic reactivity is mainly dependent on their specific surface area. A possible explanation for the lack of significant effect of the initial size of aggregates of nanosilicas on their rate of reaction is that the initial aggregation state of the nanosilica suspensions is changed after they are introduced into the environment of cement composites.

In fact, the ionic composition of pore fluid of cement based materials is entirely different from the initial ionic composition of nanosilica suspensions. In particular, pore fluid contains high concentration of multivalent cations, such as Calcium ions. It has been postulated that the Calcium ions could act as bridges between nanosilica particles, through the following reaction [1,24-25]:

$$SiO^- + Ca^{2+} + {}^-OSi \longrightarrow SiO^{-\ +}Ca^{+\ -}OSi \tag{4}$$
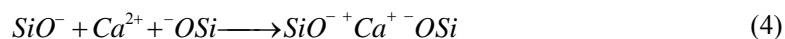
It should be noted that at the first minutes of cement hydration a considerable amount of Calcium ions are liberated into the pore fluid [27-28]. For instance, at the first 10 min of cement hydration, Labri et al. [29] reported a concentration of about 0.85g /lit Ca^{2+} ions in the pore fluid of a cement paste with a water/cement ratio of 0.45. It is notable that during the induction period, the concentration of Ca^{2+} ions increases by passing time, surpassing the theoretical level of saturation for Ca^{2+} ions [28]. The saturation level for Ca^{2+} ions is about 20mmol/lit, which corresponds to a solution with a concentration of 0.8g/lit.

To investigate the validity of the above explanation, size distribution of various suspensions of nanosilicas were determined after mixing them with appropriate amounts of Calcium Hydroxide solutions, simulating the cement paste environment with regards to Ca^{2+} ion content.
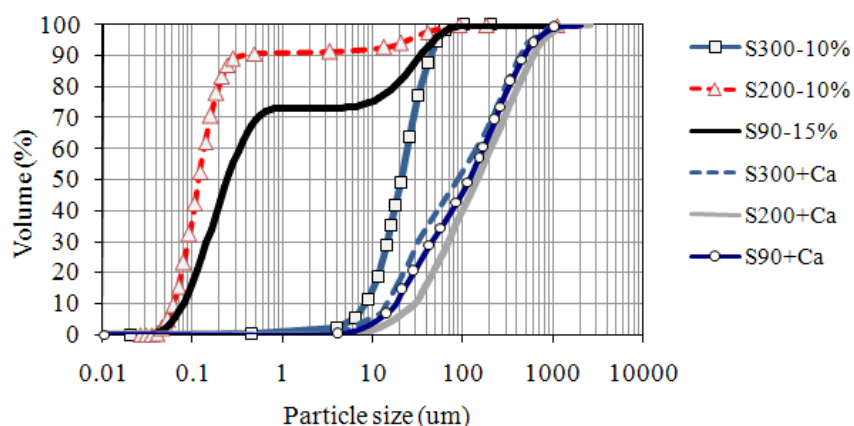
Figure 5. The influence of Ca^{2+} ions on the aggregation status of the nanosilica suspensions

In Fig. 5, the size distributions of nanosilica suspensions used in cement pastes before and after addition of Calcium ions are presented. In this figure, for instance, the abbreviation S200+Ca denotes the aggregation status of suspension of S200 after addition of Ca^{2+} ions, according to the preparation method described earlier in section 2.2. As it is shown, the addition of Calcium ions by only 0.8% of nanosilica weight leads to considerable aggregation of pyrogenic nanosilicas. After the addition of Calcium ions, the median aggregate sizes of the suspensions S90-15%, S200-10% and S300-10% changed from 0.27 μm, 0.135 μm and 22.8 μm, to 120 μm, 150 μm and 90μm, respectively. The results show that although significant differences exist between the initial size distributions of the nanosilicas, after addition of Ca^{2+} ions the aggregation status of the nanosilicas is fairly similar.

3.4. Effect of nanosilicas and silica fume on hydration degree of Portland cement

Hydration degree of cement in the cement pastes determined at different ages is shown in Fig. 6. The results indicate that cement in pastes containing the pyrogenic nanosilicas and silica fume had higher hydration degree compared to the plain paste at the first day. This means that the nanosilicas and silica fume had accelerating influence on the early hydration of cement. It appears that reduction of induction period due to fast pozzolanic reactivity of nanosilicas and the precipitation of the hydrate products on the silica surfaces accelerate the hydration of cement at the early ages and consequently leads to higher hydration degree of cement at the first day.

It is interesting to note that with the progress of hydration, the rate of cement hydration in pastes containing nanosilicas becomes lower than the plain paste. The hydration degree of cement in the cement pastes containing the nansosilicas was similar to the hydration of cement in the plain paste at 3 and 7 days and became lower at ages of 28 and 100 days.

The results show that although the effect of silica fume on cement hydration was in general similar to nanosilicas, its manifestation was somewhat slower. Silica fume accelerated cement hydration up to 7days and lowered degree of cement hydration at 28 and 100 days. It appears that the nanosilicas due to considerable aggregation in the pore fluid entrap a considerable amount of water in their structure, leadings to reduction of available water for hydration of cement [1]. It is interesting to note that the specific surface area of the nanosilicas did not significantly influence the hydration degree of cement.
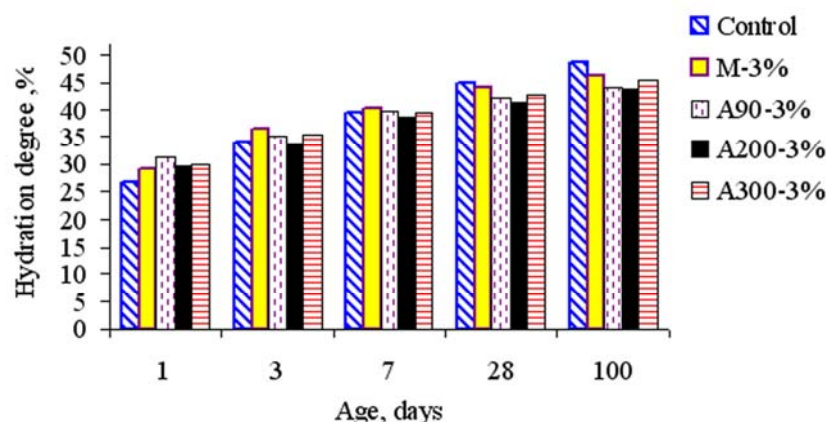
Figure 6. The hydration degree of cement in the cement pastes

3.5 Setting times

The initial and final setting times of the cement pastes were determined by the vicat needle penetration test and the results are presented in table 2. Although the tests were not made on pastes at normal consistency and the results were thus affected by difference in viscosity of the pastes, nonetheless the accelerating effect of nanosilicas in shortening the setting times is evident.

The results indicate that the nansoilicas have an accelerating influence on the initial setting time of the cement pastes while silica fume prolongs this period. Nanosilicas with higher surface areas result in shorter initial setting time of the pastes. It is also observed that the pyrogenic nanosilicas and silica fume shortened the difference between the initial and final setting times of the pastes.

It is postulated that reduction in Ca^{2+} and OH^- concentration in the pore fluid could accelerate the induction period of cement pastes [1,6,9-10]. Nanosilicas due to fast pozzolanic reactivity could reduce the concentration of Calcium and Hydroxide ions; thus, these materials could shorten the induction period. The effect of pyrogenic nanosilicas with higher specific surface areas on reducing the induction period of pastes is more pronounced due to higher rate of pozzolanic reactivity of these materials. The initial set coincides with the end of induction period [28]. Hence, reduction of initial setting times of cement pastes with increasing the surface area of the pyrogenic nanosilicas and their replacement level can be due to fast pozzolanic reactivity of nanosilicas. It is notable that similar results based on the dependence of initial setting times of cement pastes on the rate of pozzolanic reactivity of nanosilica sols were also obtained in [1].

Silica fume does not have significant pozzolanic reactivity at early ages; therefore, this material not only could not shorten the induction period and consequently initial set of pastes, but also higher initial setting times was observed due to lower cement content of the pastes containing silica fume compared to control mixture.

Table 2: Setting times of the cement pastes

Mixture ID	Initial setting (min)	Final setting (min)	Δt (min)
Control	206	298	92
A300-1%	160	219	59
A200-1%	160	220	60
A90-1%	187	248	60
M-1%	210	272	62
A300-2%	85	130	45
A200-2%	122	170	48
A90-2%	163	226	63
M-2%	210	270	60
A300-3%	58	105	47
A200-3%	75	112	48
A90-3%	145	200	55
M-3%	208	268	60
A90-5%	120	164	44
M-5%	233	284	51
M-7.5%	247	290	43

Shortening the period between initial and final setting times in the presence of nanosilicas and silica fume could be due to accelerating effect of these materials on the hydration of cement.

4. CONCLUSIONS

The results indicate that dispersed pyrogenic nanosilica suspensions are extensively coagulated in the presence of Ca^{2+} ions at concentration of these ions corresponding to the pore fluid of cement pastes. This phenomenon, which is believed to be due to the bridging effect of Ca^{2+} ions, can increase the median sizes of aggregates in the initial suspension by up to 1000 times.

The rate of pozzolanic activity of the nanosilicas in lime pastes was very high compared to silica fume. The rate of pozzolanic activity increased with increasing surface areas and Aerosil 300 with specific surface area of 300 m^2/g consumed more than 80% of lime in just 3.5 hours. A similar trend on dependence of the rate of pozzolanic reactivity of nanosilicas on their surface area was also found in the cement pastes.

The initial dimensions of nanosilica aggregates did not significantly influence their pozzolanic reactivity. This is believed to be due to the extensive coagulation of nanosilica aggregates, after they are introduced into cement composites, which results in formation of

agglomerates with relatively similar size.

The pyrogenic nanosilicas and silica fume accelerated the early hydration of cement. However, by the progress of hydration and after the 7th day, the hydration degree of cement in cement pastes containing the nanosilicas was reduced compared to the plain paste. The above mechanism could explain results reported in the literature with regards to reduced rate of strength development of cement mixtures containing nanosilicas at later ages compared to the plain mixtures.

The pyrogenic nanosilicas accelerate the initial setting time and reduce the difference between the initial and final setting times of the cement pastes.

REFERENCES

1. Madani H, Bagheri A, Parhizkar T. The pozzolanic reactivity of monodispersed nanosilica hydrosols and their influence on the hydration characteristics of Portland cement, *Cement and Concrete Research*, **43**(2012) 1563-70.
2. Bagheri A, Parhizkar T, Madani H, Raisghasemi AM. The influence of different preparation methods on aggregation status of pyrogenic nanosilicas utilized in cement mixtures, *Materials and Structures*, **46**(2013) 135-43.
3. Madani H, Bagheri A, Parhizkar T. A comparison between the pozzolanic reactivity of nanosilica sols and pyrogenic nanosilicas, *Proceeding of HiPerMat 2012 3rd International Symposium on UHPC and Nanotechnology for High Performance Construction Materials*, Kassel university press Gmbh, Kassel, 2012, pp. 125-131.
4. Brinkmann U, Ettlinger M, Kerner D, Schmoll R. Synthetic Amorphous Silica, in: Colloidal Silica, *Fundamentals and Applications*, Taylor and Francis group, Boca raton, 2006, pp. 575-588.
5. Gunko VM, Zarko VI, Leboda R, Chibowski E. Aqueous suspension of fumed oxides, particle size distribution and zeta potential, *Advances in Colloid and Interface Science*, **91**(2001) 1-112.
6. Stein HN, Stevels JM. Influence of silica on the hydration of 3CaO.SiO2, *Journal of Applied Chemistry*, **14**(1964) 338-46.
7. Kurdowski W, Nucun-Wczelik W. The tricalcium silicate hydration in the presence of active silica, *Cement and Concrete Research*, **13**(1983) 341-8.
8. Wu ZQ, young JF. The hydration of tricalcium silicate in presence of colloidal silica, *Journal of Materials Science*, **19**(1984) 3477-86.
9. Beedle S.S, Groves G.W, Rodger S.A. The effect of fine pozzolanic and other particles on hydration of C3S, *Advances in Cement Research*, **2**(1989) 3-8.
10. Korpa A, Kowald T, Trettin T. Hydration behavior, structure and morphology of hydration phases in advanced cement-based systems containing micro and nanoscale pozzolanic additives, *Cement and Concrete Research*, **38**(2008) 955-62.
11. Bjornstorm J, Martinelli A, Matic A, Borjesson L, Panas I. Accelerating effects of

colloidal nano-silica for beneficial calcium-silicate-hydrate formation in cement, *Chemical Physics Letters*, **392**(2004) 242-8.

12. Sneff L, Labrincha J.A, Ferreria V.M, Hortza D, Repette W.L. Effect of nano-silica on rheology and fresh properties of cement pastes and mortars, *Construction and Building Materials*, **23**(2008) 2487-91.

13. ASTM C1240, Standard specifications for silica fume used in cementitious mixtures, American Society for Testing and Materials, 2006.

14. Amiri A, Øye G, SjÖblem J. Influence of pH, high salinity and particle concentration on stability and rheological properties of aqueous suspensions of fumed silica, *Colloid and Interfaces A: Physicochem Engineering Aspects*, **349**(2009) 43-54.

15. Juilland P, Gallucci E, Flatt R, Scrivener K. Dissolution theory applied to the induction period in alite hydration, *Cement and Concrete Research*, **40**(2010) 831–44.

16. Papadakis V.G, Experimental investigation and theoretical modeling of silica fume activity in concrete, *Cement and Concrete Research*, **29**(1999) 79-86.

17. Neithalath N, Persun J, Hossain A. Hydration in high–performance cementitious systems containing vitreous calcium aluminosilicate or silica fume, *Cement and Concrete Research*, **39**(2009) 473-81.

18. Taylor H.F.W. *Cement Chemistry*, Thomas Telford, 2nd edition, London, 1997.

19. ASTM C191. Standard test method for time of setting of hydraulic cement by Vicat Needle. American Society for Testing and Materials, 2004.

20. Rahaman M.N. *Ceramic Processing and Sintering*, Marcell Dekker Inc, 2nd edition, New York, 2003.

21. Roberts WO. Silica Manufacturing and applications of water-borne colloidal silica, in: Colloidal Silica, Fundamentals and applications, Taylor and Francis group, Boca raton, 2006, pp. 131-176.

22. Chen S, Øye G, SjÖblem J, Effect of pH and salt on rheological properties of Aerosil suspensions, *Journal of Dispersion Science and Technology*, **28**(2007) 845-53.

23. Iler RK. *The Chemistry of Silica*, John Wiley, New York, 1979.

24. Shaw D.J. *Introduction to Colloid and Surface Chemistry*, Butterworth-Heinemann, Oxford, 2003.

25. Iler KR. Coagulation of colloidal silica by calcium ions, mechanism and effect of particle size, *Journal of Colloid and Interface Science*, **53**(1975) 476-88.

26. Zerrouk R, Foissy A, Mercier R, Chevallier Y, Morawski JC. Stady of Ca2+-induced silica coagulation by small angle scattering, *Journal of Colloid and Interface Science,* **130**(1990) 20-29.

27. Odler I. Hydration, setting and hardening of Portland cement, in: *Lea´s Chemistry of Cement and Concrete*, 4th edition, Elsevier Ltd, London, 2004, pp. 241-297.

28. Gartner EM, Young JF, Damidot DA, Jawed I. Hydration of Portland cement, in: *Structure and performance of cements, Spon Press*, New York, 2002, pp. 55-113.

29. Labri JA, Fraay ALA, Bijen JA. The chemistry of the pore solution of CSF-blended cement system, *Cement and Concrete Research*, **20**(1990) 506–16.